include both entropic effects and stabilizing interactions between atoms in the link sequence and the rest of the protein. As only some of these free energy components can be quantified at present, it is not yet possible to partition the stabilization energy into its component terms (*15, 16*).

The free energy associated with the transition from the unfolded, random coil state to the folded, helical state for α_4 in the absence of denaturants could be estimated by methods that involve extrapolation to zero GuHCl concentration (*17*); the free energy associated with the folding process was calculated to be -22 kcal mol^{-1} (*18*). Although this value is approximate because of the assumptions invoked in the development of linear free energy models (*17, 19*), it allows comparison of α_4 with other small, natural proteins that have been analyzed in the same way (Table 1) (*20*). α_4 possesses considerable stability when compared with other small proteins and thus provides a stable framework for the incorporation of future design modifications.

It is reasonable to adopt the working assumption that α_4 contains four closely packed α-helical segments. Additional chemical, crystallographic, and spectroscopic investigations are necessary to determine the arrangement of the helices and the positions of the loops in the structure.

REFERENCES AND NOTES

1. W. F. DeGrado, *Adv. Prot. Chem.*, in press; J. S. Richardson and D. C. Richardson, in *Protein Engineering*, D. L. Oxender and C. F. Fox, Eds. (Liss, New York, 1987), pp. 149–163; E. T. Kaiser and F. J. Kézdy, *Science* **223**, 249 (1984); M. Mutter, *Angew. Chem. Int. Ed. Engl.* **24**, 639 (1985); R. Moser *et al.*, *ibid.*, p. 719 (1985); C. O. Pabo, *Nature* **301**, 200 (1983); M. Mutter, K.-H. Altman, T. Z. Vorherr, *Naturforsch* **41b**, 1315 (1986).
2. D. Eisenberg *et al.*, *Proteins Struct. Funct. Genet.* **1**, 16 (1986).
3. S. P. Ho and W. F. DeGrado, *J. Am. Chem. Soc.* **109**, 6751 (1987).
4. W. F. DeGrado, L. J. Regan, S. P. Ho, *Cold Spring Harbor Symp. Quant. Biol.*, in press.
5. K. Shoemaker *et al.*, *Nature* **326**, 563 (1987).
6. P. C. Weber and F. R. Salemme, *ibid.* **287**, 82 (1980); P. Argos, M. G. Rossman, J. E. Johnson, *Biochem. Biophys. Res. Commun.* **75**, 83 (1977); S. Sheriff, W. A. Hendrickson, J. L. Smith, *J. Mol. Biol.* **197**, 273 (1987); B. C. Finzel, P. C. Weber, K. D. Hardman, F. R. Salemme, *ibid.* **186**, 627 (1985).
7. C. Chothia, M. Levitt, D. Richardson, *Proc. Natl. Acad. Sci. U.S.A.* **74**, 4130 (1977); C. Chothia, *Annu. Rev. Biochem.* **53**, 537 (1984).
8. D. E. Blagdon and M. Goodman, *Biopolymers* **14**, 241 (1975).
9. G. D. Rose *et al.*, *Adv. Prot. Chem.* **37**, 1 (1985).
10. K. Knight and R. T. Sauer, unpublished results.
11. W. W. Burnette, *Anal. Biochem.* **112**, 195 (1981).
12. S. Y. M. Lau, A. K. Taneja, R. S. Hodges, *J. Biol. Chem.* **259**, 13253 (1984).
13. N. Greenfield and G. D. Fasman, *Biochemistry* **8**, 4108 (1969).
14. When GuHCl denaturation curves are measured at different concentrations of peptide, the same rank order of stability as shown in Fig. 5 is observed at all physically reasonable peptide concentrations. The precise midpoint of the denaturation curve is, of course, dependent on the concentrations of α_1 and α_2 (*3*).
15. M. I. Page and W. P. Jencks, *Proc. Natl. Acad. Sci. U.S.A.* **68**, 1678 (1971).
16. C. R. Cantor and P. R. Schimmel, *Biophysical Chemistry* (Freeman, San Francisco, 1980), vol. 1, pp. 283–285.
17. J. A. Schellman, *Biopolymers* **17**, 1305 (1978).
18. To estimate the stability of protein α_4 in the absence of denaturant, measurements were made in the region near the midpoint of the transition of the GuHCl denaturation curve. From these data, either by linear extrapolation to zero GuHCl or by multiplying the slope by the midpoint (*16*), values of -22.4 kcal mol^{-1} or -22.5 kcal mol^{-1}, respectively, were calculated for the free energy of folding in the absence of denaturant.
19. C. N. Pace, *Biochemistry* **28**, 288 (1979); F. Ahmad and C. C. Bigelow, *Biopolymers* **25**, 1623 (1986).
20. F. Ahmad and C. C. Bigelow, *J. Biol. Chem.* **257**, 12935 (1982); C. N. Pace, *CRC Crit. Rev. Biochem.* 1 (1975).

21. We thank K. Knight and R. T. Sauer for their generous gift of plasmid pTM201/NS3-3; L. Janvier for conducting amino acid analysis; B. Krieger for Edman sequencing and S. Ho for the chemical synthesis of α_4; her preliminary spectroscopic and thermodynamic experiments on this material encouraged us in our work. Also we thank D. Eisenberg, S. Ho, D. Oprian, F. R. Salemme, P. Weber, and Z. Wasserman for helpful advice on various aspects of this work. We dedicate this report to the memory of Professor E. T. Kaiser of Rockefeller University.

29 April 1988; accepted 16 June 1988

Coordinate Hormonal and Synaptic Regulation of Vasopressin Messenger RNA

FRANK BALDINO, JR.,* TERESA M. O'KANE, SANDRA FITZPATRICK-MCELLIGOTT, BETTY WOLFSON

Previous studies have shown that adrenalectomy augments arginine vasopressin (AVP) messenger RNA levels in the adult paraventricular nucleus. It is now demonstrated that unilateral lesions in the lateral septal nucleus enhance the adrenalectomy-induced expression of AVP mRNA. This effect was entirely ipsilateral to the lesion and most prominent in the rostral paraventricular nucleus and related nuclei. Moreover, AVP and AVP mRNA were found to be colocalized with oxytocin in a few neurons. These results indicate that mRNA expression is modulated by synaptic influences and raise the possibility that synaptically mediated selection of neuronal phenotypes is a dynamic feature of the mature central nervous system.

THE EXPRESSION OF AVP MRNA within several subdivisions of the paraventricular nucleus (PVN) is regulated by glucocorticoids (*1–6*). Adrenalectomy induces the expression of AVP mRNA in corticotropin-releasing factor (CRF)–immunoreactive neurons within the PVN (*1, 2*), illustrating the potential of the adult genome to be differentially regulated in response to hormonal challenge. Other physiological influences, however, have also been reported to alter gene expression. The transmitter phenotype produced in developing peripheral ganglionic neurons (*7*), as well as the synthesis of specific muscle proteins (*8*), has been shown to depend, in part, on the type of presynaptic innervation. These findings suggest that synaptic input influences phenotypic expression in target tissues. The purpose of this study was to determine whether specific afferents contribute to the plasticity in AVP expression induced by adrenalectomy. We now report that the adrenalectomy-induced expression of AVP mRNA in the PVN can be enhanced by reducing specific afferent synaptic input.

Adrenalectomized (14-day-old; $n = 25$) and sham-operated ($n = 10$) male Sprague-Dawley rats were subjected to a unilateral electrolytic lesion in one of a number of regions shown by anatomical and physiological studies to project to the PVN (*9–15*). These regions included the bed nucleus of the stria terminalis, several subdivisions of the lateral septal nucleus, and the hippocampus (including the subiculum). The ipsilateral nature of these projections permitted the side contralateral to the lesion to serve as a control in each section. The anatomical locations of all lesions were verified histologically. In some experiments ($n = 6$), dexamethasone pellets (120 μg/day for 7 days) were administered subcutaneously 7 days after adrenalectomy.

In animals with lateral septal lesions, the number of neurons expressing AVP mRNA was increased in the rostral half of the PVN on the side ipsilateral to the lesion (Fig. 1). Most notably, AVP mRNA was detected in a population of neurons that normally do not express AVP or AVP mRNA. These

Medical Products Department, Experimental Station, E. I. du Pont de Nemours & Company, Wilmington, DE 19898.

*To whom correspondence should be sent at Cephalon, Inc., 145 Brandywine Parkway, West Chester, PA 19380.

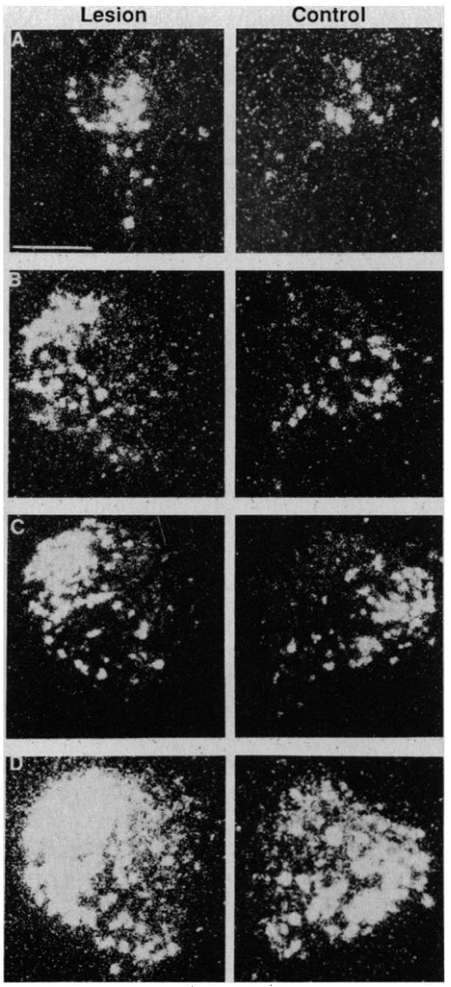

Fig. 1. Dark-field photomicrographs depicting the distribution of AVP mRNA at four selected levels in the PVN. Sections were prepared from adrenalectomized rats that had received unilateral septal lesions. The sections are arranged rostral to caudal (**A** to **D**) with the left panels illustrating the side of the lesion. A higher density of neurons with hybridized message is seen in all sections ipsilateral to the lesion. In (A to C) this increase in labeled neurons is located ventromedially on the lesioned side. In (C), an increased density of labeled neurons is present laterally and dorsally on the lesioned side. The caudal extent of this asymmetry is noted in (D). Bar, 200 μm. A 24-base oligodeoxynucleotide probe complementary to the glycoprotein coding region of AVP mRNA was prepared according to previously described methods (*1, 2, 20*). The specific activity of the ^{125}I-labeled probe was approximately 10^8 cpm μg^{-1}. Colchicine (75 μg)-treated rats were perfusion-fixed and their brains transversly sectioned at 30 μm. In situ hybridization histochemistry was performed as described (*1, 2, 20*). For autoradiography, slides were dipped in Kodak NTB2 emulsion diluted 1:1 with distilled H_2O. Slides were exposed for 4 days in lightproof boxes at 4°C. Development was performed with Kodak-D19 for 2 min at 16°C; slides were washed in distilled H_2O for 30 s, and this was followed by 5-min fixation with Kodak fixer at 16°C. The fixed samples were then washed in distilled H_2O for 30 min, dehydrated, and protected by cover slips.

neurons were located within the ventral medial portion of the posterior magnocellular and medial parvocellular subdivisions of the PVN extending to the border of the third ventricle. Asymmetric distributions of neurons containing AVP mRNA were also observed in more scattered populations of neurons in the periventricular region, the lateral portion of the posterior magnocellular subdivision, the accessory PVN, and a narrow band of neurons extending over the dorsal aspect of the fornix. The distribution of AVP mRNA on the nonlesioned side was identical to that seen after adrenalectomy alone (*1*). Lesions of the ventral and lateral-intermediate regions of the lateral septal nucleus extending ventrally to the anterior commissure were most effective in inducing this asymmetry. In contrast, lesions placed in dorsal or medial portions of this nucleus did not produce these effects.

The asymmetrical distribution of AVP mRNA was precisely paralleled by the distribution of AVP immunoreactivity. Consistent with in situ hybridization, septal lesion resulted in a 56% increase in the number of AVP-immunoreactive neurons in the rostral half of the PVN on the side ipsilateral to the lesion (Fig. 2). The magnitude and extent of this asymmetry were determined by counting individual neurons in each section throughout the rostral to caudal extent of the PVN in three individual cases. The neuronal distribution of AVP in the supraoptic and suprachiasmatic nuclei and the nucleus circularis remained unaltered by the septal lesion.

A portion of the newly labeled population of AVP-immunoreactive neurons overlaps that reported for oxytocin neurons (*16, 17*).

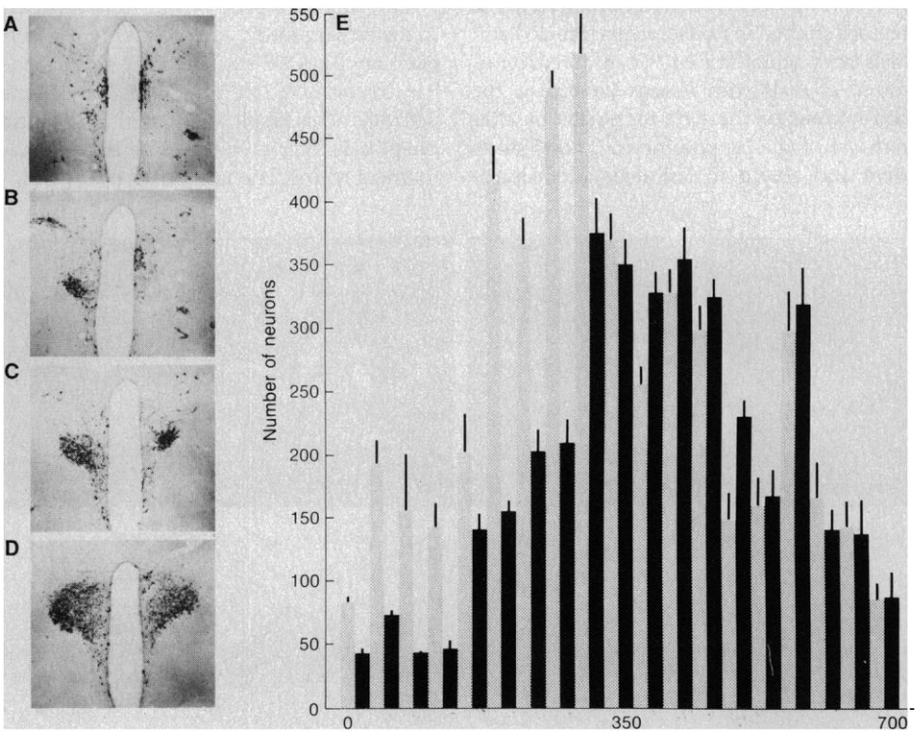

Fig. 2. (**A** to **D**) Bright-field photomicrographs illustrating the distribution of AVP-immunoreactive neurons at four selected levels of the PVN. Sections are arranged rostral to caudal (**A** to **D**). The left sides of these panels are ipsilateral to the septal lesion. On the left side of (A), a population of AVP-immunoreactive neurons is apparent in the medial ventral portion of this nucleus that is not present on the right side. The number of immunoreactive neurons constituting this new AVP population increases in (B) and (C) and expands in a dorsal to ventral direction. Also, the density of immunoreactive neurons is dramatically enhanced in a narrow band of cells dorsal to the fornix [left sides of (B) and (C)]. (D) An increased number of immunoreactive neurons is evident in the ventral and lateral portions of the nucleus. A scattered population of neurons in the medial and periventricular region of this nucleus is also evident in (A) to (D). (**E**) Bar graph illustrating the mean (± SD; n = 3 cases) number of AVP-immunoreactive neurons on each side of the brain. Neurons in serial 20-μm sections are plotted as a function of their anterior to posterior (A–P) location within the PVN. Neurons on the lesioned side are depicted by the stippled bars; those on the nonlesioned side are shown in black. The A–P level in (A) represents A–P zero on the bar graph. The number of neurons indicated on the ordinate was corrected by the method of Abercrombie (*21*) and represents 120% of the actual number of immunoreactive neurons in these sections. The vasopressin antiserum was a rabbit polyclonal (Immuno Nuclear) and was used in a 1/2000 dilution. The antiserum was completely adsorbed with AVP (1 μg/ml), and the signal was not diminished after incubation with oxytocin (1 μg/ml).

In fact, AVP mRNA was detected within the cytoplasm of a few oxytocin-immunoreactive neurons (Fig. 3, C and D). Moreover, AVP and oxytocin immunoreactivity appeared to be colocalized in some neurons on the side ipsilateral to the lesion (Fig. 3, A and B). These peptides were most frequently found in neurons in the perifornical region and accessory PVN. A few scattered neurons were found within the defined borders of the PVN. However, expression of AVP in oxytocin neurons cannot solely account for this increased AVP population; only a few neurons appeared to contain both peptides. Nonetheless, these results suggest that the nervous system possesses the ability to induce peptide synthesis de novo in response to specific synaptic events. Oxytocin immunoreactivity in the supraoptic nucleus and anterior commissural nucleus was not influenced by these treatments.

No observable difference in the distribution of AVP or AVP mRNA occurred in the regions studied in nonadrenalectomized animals with septal lesions, or in adrenalectomized animals with lesions limited to the bed nucleus of the stria terminalis or after removal of the hippocampus. These effects were also absent in lesioned, adrenalectomized animals treated with dexamethasone.

The results of this study demonstrate that a lesion in the ventral lateral septum enhances the adrenalectomy-induced expression of AVP mRNA in the PVN. Previous physiological studies have demonstrated that AVP can enhance CRF-induced corticosterone release (*18*). The adrenalectomy-induced elevation of AVP, and the colocalization of AVP with CRF is likely to be the anatomical correlate of this effect. It has also been demonstrated that ablation of the septum results in an increase of stress-induced corticosterone levels (*19*). This result is consistent with the elevation in AVP expression demonstrated in this study.

We have previously shown that glucocorticoid levels regulate the expression of AVP mRNA in a subset of AVP neurons in the PVN (*1, 2*). A decrease in this particular class of steroid appears to increase the potential for altering the expression of the propressophysin gene within this nucleus. In the present study, adrenalectomy-induced plasticity in AVP expression is further enhanced by ablation of a specific afferent pathway. This result suggests that synaptic events may interact with the hormonal environment to regulate neuronal phenotypes.

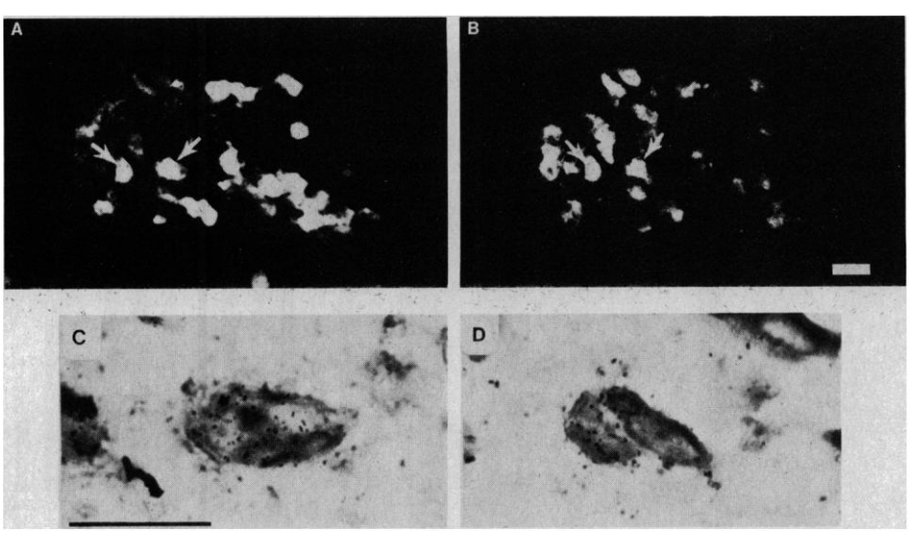

Fig. 3. Fluorescence photomicrographs demonstrating the colocalization of (**A**) oxytocin- and (**B**) AVP-immunoreactive material within the same neuron in a 25-μm section ipsilateral to the septal lesion. Arrows point to individual neurons within the perifornical region, which are unambiguously labeled with antisera directed against AVP and oxytocin. Bar, 50 μm. Specific labeling is depicted only by the brightest cells in each of these photos. (**C** and **D**) Bright-field photomicrographs of oxytocin-immunoreactive neurons containing AVP mRNA. Silver grains are shown within the cytoplasm of these neurons. Bar, 50 μm. Colocalization of these two peptides was not observed on the side contralateral to the septal lesion. For colocalization studies, animals were perfused with 4% paraformaldehyde in a variable *p*H, two-step procedure (*6*). The antisera used in this study were completely adsorbed with 1 μg of the respective peptide per milliliter. The immunoreactivity observed with either antibody was not influenced by incubation in 5 μg of the alternate peptide per milliliter. Immunohistochemistry for AVP was done in the presence of oxytocin (1 μg/ml), and that for oxytocin was done in the presence of AVP (1 μg/ml). The oxytocin antisera were raised in rabbits and used in a 1/2000 dilution. The signal was localized with rhodamine-labeled goat antibody to rabbit immunoglobulin G (IgG) (American Qualex). A mouse-derived monoclonal antibody to AVP (*22*) was visualized with fluorescein isothiocyanate–conjugated goat antibody to mouse IgG (American Qualex). No labeling was observed when either goat secondary IgG was incubated with the alternate species primary antigen.

The specificity of these effects is remarkable in light of the extensive convergence of afferent synaptic pathways onto the PVN (*9–13*). The inability of lesions in the bed nucleus or in the subiculum to alter AVP expression suggests that these inputs project to different neurons within the PVN or, under these conditions, that only certain synapses influence the expression of AVP. On the other hand, the expression of AVP in a few oxytocin-immunoreactive neurons in adrenalectomized animals with lateral septal lesions, in addition to the localization of AVP in CRF neurons, suggests that changes in neuronal phenotype consequent to specific hormonal and synaptic influences can occur in biochemically distinct populations of neurons in the adult central nervous system.

Several studies have reported that septal fibers (*10, 12, 15*) and functional septal synapses (*9–13*) are distributed on both AVP and oxytocin neurons in the PVN. In our study, the effects were limited to a discrete population of hypothalamic neurons at the rostral level of the PVN. It is uncertain whether this differential influence of synaptic input reflects differences in the factors released at each synapse or differences in the physiological effects produced by this input. Furthermore, since numerous fiber tracts traverse or are in close proximity to the lesioned area, it cannot be determined whether direct, monosynaptic projections from the lateral septum are responsible for these effects. Nonetheless, afferents to the PVN arising from, or passing through, the ventral septum are responsible for the asymmetries reported here. These results suggest that the scope of synaptic interactions that occur between afferent projections and the hypothalamus include an interaction between synapse and genome.

These experiments may recapitulate a developmental process that differentiates the AVP phenotype. Alternatively, it is possible that a component of the information that is signaled synaptically between adult neurons regularly includes information that can modulate gene expression. The latter possibility suggests that synaptically mediated selection of neuronal phenotypes may be a normal feature of the mature central nervous system.

REFERENCES AND NOTES

1. B. Wolfson, R. W. Manning, L. G. Davis, R. Arentzen, F. Baldino, Jr., *Nature* **315**, 59 (1985).
2. L. G. Davis *et al.*, *Proc. Natl. Acad. Sci U.S.A.* **83**, 1145 (1986).
3. K. A. Roth, E. Weber, J. D. Barchas, *Life Sci.* **31**, 1957 (1982).
4. G. Tramu, C. Croix, A. Pillez, *Neuroendocrinology* **37**, 467 (1983).
5. J. Z. Kiss, E. Mezey, L. Skirboll, *Proc. Natl. Acad. Sci. U.S.A.* **81**, 1854 (1984).

6. P. E. Sawchenko, L. W. Swanson, W. W. Vale, *ibid.*, p. 1883.
7. P. A. Walicke *et al.*, *ibid.* **74**, 5867 (1977).
8. G. Salviati, E. Biasi, M. Aloisi, *Nature* **322**, 637 (1986).
9. D. A. Poulain, R. Ellendorff, J. D. Vincent, *Neuroscience* **5**, 379 (1980).
10. A. J. Silverman, D. L. Hoffman, E. A. Zimmerman, *Brain Res. Bull.* **6**, 47 (1981).
11. A. J. Silverman and B. J. Oldfield, *Peptides* **5**, 139 (1984).
12. E. Tribollet and J. J. Dreifuss, *Neuroscience* 6, 1315 (1981).
13. Q. J. Pittman, H. W. Blume, L. P. Renaud, *Brain Res.* **215**, 5 (1981).
14. D. Saphier and S. Feldman, *Neuroscience* **20**, 749 (1987).
15. B. J. Oldfield and A. J. Silverman, *Brain Res. Bull.* **14**, 143 (1985).
16. P. E. Sawchenko and L. W. Swanson, *J. Comp. Neurol.* **205**, 260 (1982).
17. C. N. Rhodes, J. I. Morrell, D. W. Pfaff, *ibid.* **198**, 45 (1981).
18. G. E. Gillies, R. A. Linton, P. T. Lowry, *Nature* **299**, 355 (1982).
19. J. Seggie, I. Uhlir, G. M. Brown, *Neuroendocrinology* **16**, 225 (1974).
20. M. E. Lewis, R. Arentzen, F. Baldino, Jr., *J. Neurosci. Res.* **16**, 117 (1986).
21. M. Abercrombie, *Anat. Rec.* **94**, 239 (1946).
22. A. Hou-Yu *et al.*, *J. Histochem. Cytochem.* **30**, 1249 (1982).
23. We thank J. M. Reid for technical assistance, J. P. Lancaster and R. P. Meade for photographic assistance, and J. P. Card, M. E. Lewis, R. G. Siman, and M. J. Gutnick for critical evaluation of the manuscript. We also gratefully acknowledge S. J. Watson for providing the oxytocin antisera, A. Hou-Yu for providing the monoclonal antibody to AVP, and P. Sawchenko for advice with immunocytochemistry.

29 December 1987; accepted 10 June 1988

NMDA Receptor Losses in Putamen from Patients with Huntington's Disease

ANNE B. YOUNG,* J. TIMOTHY GREENAMYRE, ZANE HOLLINGSWORTH, ROGER ALBIN, CONSTANCE D'AMATO, IRA SHOULSON, JOHN B. PENNEY

N-Methyl-D-aspartate (NMDA), phencyclidine (PCP), and quisqualate receptor binding were compared to benzodiazepine, γ-aminobutyric acid (GABA), and muscarinic cholinergic receptor binding in the putamen and cerebral cortex of individuals with Huntington's disease (HD). NMDA receptor binding was reduced by 93 percent in putamen from HD brains compared to binding in normal brains. Quisqualate and PCP receptor binding were reduced by 67 percent, and the binding to other receptors was reduced by 55 percent or less. Binding to these receptors in the cerebral cortex was unchanged in HD brains. The results support the hypothesis that NMDA receptor–mediated neurotoxicity plays a role in the pathophysiology of Huntington's disease.

HUNTINGTON'S DISEASE (HD) IS AN autosomal dominant inherited disorder characterized by progressive cognitive decline and involuntary movements starting in mid-life (*1*). Genetic linkage studies have localized the HD gene to the tip of chromosome 4, but the actual gene has not been isolated, and the HD biochemical defect is still unknown (*2*). Pathologically, HD is characterized by extensive neuronal loss in the caudate nucleus and putamen, and relative sparing of neurons in the rest of the brain (*3*). Striatal afferent pathways are largely spared. Among the neurochemical correlates of striatal neuron loss are decreases in striatal glutamate decarboxylase (GAD) activity, GABA, and substance P (*4*). Kainate, the glutamate agonist and neurotoxin, produces a loss of GABA and GAD when it is injected into rodent striata; afferent terminals and fibers of passage are spared. It was hypothesized that HD may be due to a genetic susceptibility to an exogenous or endogenous neurotoxin (*5*). The kainate model for HD became less attractive, however, when kainate was found to destroy all striatal neurons, whereas, in HD striatum, certain neurons were spared (*6*). Striatal injections of quinolinic acid, an endogenous neurotoxin, produced both the GABA losses and the selective sparing seen in HD (*7*). Although these findings have been challenged (*8*), studies in rodents and primates support the original observation (*9*). Quinolinic acid exerts its effects through a subtype of excitatory amino acid receptor, the *N*-methyl-D-aspartate (NMDA) receptor; NMDA receptor antagonists block quinolinate neurotoxicity (*9, 10*).

If NMDA receptors are involved in the pathogenesis of HD, cells with high densities of NMDA receptors should be preferentially lost in HD striatum, and NMDA receptor density should decline concommitantly. We examined this possibility by measuring NMDA and other receptors in cerebral cortex and putamen from HD brains.

Blocks of tissue were cut from frozen coronal sections through midputamen and globus pallidus of HD and control brains. The blocks included insular cortex and were coded and assayed by persons blind to the clinical diagnosis (*11*). In initial experiments, [^{3}H]glutamate binding to NMDA-sensitive and quisqualate-sensitive binding sites was measured. Sections from seven HD and six control brains (*11*) were washed with cold buffer for 30 min and then incubated in 20 n*M* [^{3}H]glutamate and 50 m*M* tris-HCl buffer, *p*H 7.2, containing 2.5 m*M* $CaCl_2$, with or without 100 μ*M* NMDA, 2.5 μ*M* quisqualate, 100 μ*M* NMDA plus 2.5 μ*M* quisqualate, or 1 m*M* glutamate as a blank (*12*).

[^{3}H]Flunitrazepam binding to benzodiazepine receptors, [^{3}H]muscimol binding to GABA receptors, and [^{3}H]quinuclidinyl benzilate binding to muscarinic cholinergic receptors were measured in the same group of brains (*11, 13*). All sections were placed in x-ray cassettes with appropriate standards, apposed to tritium-sensitive Ultrofilm ^{3}H (LKB), exposed for 1 to 6 weeks, and developed and analyzed by computer-assisted densitometry (*12, 13*). Five to eight readings in each area were averaged. Insular cortex and putamen were examined; caudate nucleus was too small to analyze reliably.

In control putamen, NMDA (100 μ*M*) competed for only 15% of total glutamate binding in tris-HCl–$CaCl_2$ buffer; quisqualate (2.5 μ*M*) competed for 35% (*14*). In cerebral cortex, 25% of total glutamate binding was NMDA sensitive and 50% was quisqualate sensitive. In HD putamen, both total glutamate and quisqualate-sensitive binding were reduced 67% in HD brains compared to control. The NMDA-sensitive binding was reduced 95% in HD compared to controls (Fig. 1). In this group of brains, there were significant but smaller decreases in muscarinic cholinergic (50%), $GABA_A$ (55%), and benzodiazepine receptors (55%) in HD putamen. The decreases in NMDA receptors were not statistically significant as compared to other receptors [$P < 0.07$, Kruskal-Wallis nonparametric one-way analysis of variance (ANOVA)]. Insular cortex receptor binding for all ligands was normal in HD brains.

Because only 15% of glutamate binding in tris-HCl–$CaCl_2$ buffer was sensitive to NMDA, we examined an additional five HD and six control brains (*11*) with the assay described above, as well as with two more specific assays for the NMDA receptor complex. In one assay for NMDA receptors,

A. B. Young, J. T. Greenamyre, Z. Hollingsworth, R. Albin, J. B. Penney, Department of Neurology, University of Michigan, Ann Arbor, MI 48109.
C. D'Amato, Department of Pathology, University of Michigan, Ann Arbor, MI 48109.
I. Shoulson, Department of Neurology, University of Rochester, Rochester, NY 14642.

*To whom correspondence should be addressed at Neuroscience Building, 1103 East Huron Street, Ann Arbor, MI 48104.